the plant journal

SEB Society for Experimental Biology

The Plant Journal (2012) **71**, 824–835 doi: 10.1111/j.1365-313X.2012.05034.x

Role of pectin methylesterases in cellular calcium distribution and blossom-end rot development in tomato fruit

Sergio T. de Freitas[1], Avtar K. Handa[2], Qingyu Wu[3], Sunghun Park[3] and Elizabeth J. Mitcham[1,*]

[1]*Department of Plant Sciences, University of California, Davis, CA 95616, USA,*

[2]*Department of Horticulture and Landscape Architecture, Purdue University, West Lafayette, IN 47907, USA, and*

[3]*Department of Horticulture, Forestry & Recreation Resources, Kansas State University, Manhattan, KS 66506, USA*

Received 8 February 2011; revised 19 April 2012; accepted 23 April 2012; Published online 28 June 2012.

*For correspondence (e-mail ejmitcham@ucdavis.edu).

SUMMARY

Blossom-end rot (BER) in tomato fruit (*Solanum lycopersicum*) is believed to be a calcium (Ca^{2+}) deficiency disorder, but the mechanisms involved in its development are poorly understood. Our hypothesis is that high expression of pectin methylesterases (PMEs) increases Ca^{2+} bound to the cell wall, subsequently decreasing Ca^{2+} available for other cellular functions and thereby increasing fruit susceptibility to BER. The objectives of this study were to evaluate the effect of *PME* expression, and amount of esterified pectins and Ca^{2+} bound to the cell wall on BER development in tomato fruit. Wild-type and *PME*-silenced tomato plants were grown in a greenhouse. At full bloom, flowers were pollinated and Ca^{2+} was no longer provided to the plants to induce BER. Our results show that suppressing expression of PMEs in tomato fruit reduced the amount of Ca^{2+} bound to the cell wall, and also reduced fruit susceptibility to BER. Both the wild-type and *PME*-silenced fruit had similar total tissue, cytosolic and vacuolar Ca^{2+} concentrations, but wild-type fruit had lower water-soluble apoplastic Ca^{2+} content and higher membrane leakage, one of the first symptoms of BER. Our results suggest that apoplastic water-soluble Ca^{2+} concentration influences fruit susceptibility to Ca^{2+} deficiency disorders.

Keywords: cell wall, PME, Ca^{2+}, calcium deficiency, disorder, tomato.

INTRODUCTION

Calcium (Ca^{2+}) is an essential plant nutrient required for cell wall structure, cellular signaling responses, and membrane function, and serves as a counter-cation inside storage organelles (White and Broadley, 2003; Hepler, 2005). Calcium deficiency disorders have been observed in many plant species, affecting quality and yield, and contributing to economic losses of crop plants (White and Broadley, 2003). Blossom-end rot (BER) is believed to be a Ca^{2+} deficiency disorder in tomato fruit (White and Broadley, 2003; Uozumi *et al.*, 2012). As in other plant species, and after many years of research, the mechanisms that lead to BER development remain poorly understood. From the late 1800s to the early 1940s, BER was believed to be caused by parasitic organisms, chemical toxicity, high plant transpiration, or lack of moisture (Wedgworth *et al.*, 1926; Chamberlain, 1933). Since the 1940s, studies have suggested that BER is a Ca^{2+} deficiency disorder in tomato fruit based on the facts that: (i) plants grown under low Ca^{2+} conditions have high risk of BER incidence; (ii) fruit with BER have a high probability of having low total tissue Ca^{2+} content; and (iii) spraying plants with Ca^{2+} reduces the risk of BER development (Ho *et al.*, 1993; Paiva *et al.*, 1998; Ho and White, 2005; Uozumi *et al.*, 2012). However, other evidence suggests that total fruit tissue Ca^{2+} content *per se* may not be the only cause of BER development. Quite often, fruit with BER have equal or higher Ca^{2+} concentrations than sound fruit (Castro, 1980; Nonami *et al.*, 1995; Saure, 2001). In addition, no threshold of fruit Ca^{2+} concentration has been used to accurately predict BER development (Saure, 2001). This finding suggests that BER may also be triggered by abnormal cellular Ca^{2+} partitioning and distribution that leads to a cellularly localized Ca^{2+} deficiency.

The sequence of events preceding BER development is increasing membrane leakage, cell plasmolysis, and membrane breakdown that lead to the water-soaked symptoms on the blossom-end fruit surface (Saure, 2001; Suzuki *et al.*, 2003; Ho and White, 2005). Increased membrane leakage has been reported to result from lower levels of free apoplastic Ca^{2+}, which stabilizes cell membranes by bridging phosphate and carboxylate groups of phospholipids and proteins at the membrane surface (Clarkson and Hanson, 1980; Legge *et al.*, 1982; Kirkby and Pilbeam, 1984; Hirschi, 2004). Previous studies have shown that apoplastic levels of Ca^{2+} must

be maintained at certain thresholds to avoid excessive membrane leakiness and damage (Hanson, 1960; Kirkby and Pilbeam, 1984; Picchioni *et al.*, 1998). Based on these ideas, BER could be triggered by an abnormal regulation of cellular Ca^{2+} partitioning and distribution that depletes the apoplastic pool of Ca^{2+} that otherwise might bind to and stabilize the plasma membrane.

The cell wall is the biggest pool of Ca^{2+} in plant tissue, reaching about 60–75% of the total tissue Ca^{2+} content (Demarty *et al.*, 1984). Pectin methylesterases (PMEs) are enzymes that de-esterify pectins, creating carboxyl groups that, at typical apoplastic pH values between 6 to 7 (Ruan *et al.*, 1995; Domingos and Huber, 1999), can form very strong intermolecular interactions with Ca^{2+} in the cell wall pectin network (Demarty *et al.*, 1984; Ralet *et al.*, 2001; Bosch and Hepler, 2005). Solutions that contain pectin and Ca^{2+} can have a total Ca^{2+}: pectin-bound Ca^{2+} ratio close to one, depending on the amount of pectin carboxyl groups, pH and Ca^{2+} concentration (Tibbits *et al.*, 1998).

In 'Rutgers' tomato fruit, *PME* expression begins at about 10 to 15 days after pollination, which correlates well with PME protein content and activity, and expression increases steadily until 30 days after pollination and declines thereafter (Harriman *et al.*, 1991). The time of increase in *PME* expression and activity precisely coincides with the critical period for BER development in tomato fruit, which also starts at about 10 to 15 DAP (Ho and White, 2005). This evidence suggests that increasing *PME* expression and activity increases pectin-localized Ca^{2+} binding sites, possibly reducing the level of apoplastic free Ca^{2+} that could bind to and stabilize the plasma membrane. This situation may increase membrane leakiness and the probability of BER development under conditions of low fruit Ca^{2+} uptake. In this case, reduction in *PME* expression and activity may directly reduce total fruit Ca^{2+} demand and, as a consequence, fruit susceptibility to BER development.

We have tested this hypothesis by examining BER development in fruits with genetically reduced levels of *PME* expression and determining its correlation with changes in cellular Ca^{2+} partitioning and distribution in fruit. We report herein that reduced *PME* expression significantly alters the levels of Ca^{2+} bound to insoluble pectin with concomitantly marked reduction in the incidence of BER in tomato fruits. These results provide an insight into the role of Ca^{2+} partitioning and distribution in BER in particular and a mechanism/method to alter highly regulated Ca^{2+} partitioning and distribution in plant tissues in general to overcome Ca^{2+} deficiency associated disorders in crops.

RESULTS

Fruit susceptibility to BER development

Throughout fruit growth and development, *PME*-silenced fruit had a lower BER incidence and electrolyte leakage in the blossom-end pericarp tissue than wild-type fruit tissue (Figure 1a,b). While more than 80% of WT (wild-type) fruit exhibited BER, only about 30% of PME-silenced fruits were affected by this disorder by the time fruit reached full size (45 DAP). *PME*-silenced fruit also had higher total water-soluble Ca^{2+} concentration in the pericarp tissue than wild-type fruit at 45 DAP (Figure 2a). The apoplastic water-soluble Ca^{2+} concentration in the pericarp tissue was also higher in *PME*-silenced than in wild-type fruit at 30 and 45 DAP (Figure 2b). Electron microscopy images show cell plasmolysis in visually healthy-appearing pericarp tissue of wild-type fruit (Figure 3a), compared with cells in the pericarp tissue of *PME*-silenced fruit, which do not show plasmolysis (Figure 3b).

Pectin methylesterase expression during fruit growth and development

The expression of the six *PME* genes PMEU1, LOC544090, LOC544289, Les.9028, Les.10790, and Les.10560 in the wild-type pericarp tissue increased 62, 491, 220, 77, 40, and 57 fold, respectively, from 15 DAP to 45 DAP (Figure 4). *PME*-silenced fruit also showed increased expression of all six *PME* genes during growth and development. However, expression of PMEU1, LOC544090, LOC544289, Les.9028, Les.10790, and Les.10560 were 48-, 474-, 214-, 63-, 18-, and

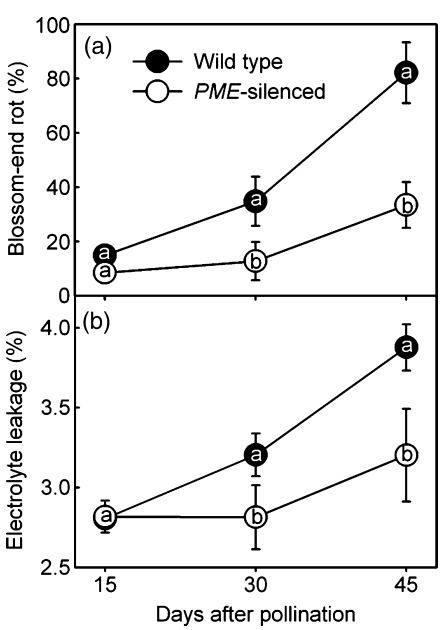

Figure 1. Silencing *PME* expression lowers tomato fruit susceptibility to BER development and electrolyte leakage of fruit pericarp tissue.
Blossom-end rot incidence (a) and electrolyte leakage of pericarp tissue (b) of wild-type and *PME*-silenced tomato fruit cultivar Rutgers. Wild-type (n = 4) and *PME*-silenced (n = 4) samples were compared by one-tailed unpaired Student's t-test. Different letters on each evaluation day represent a statistical difference between wild-type and *PME*-silenced samples (P-value < 0.05). Data are means ± standard error (SE).

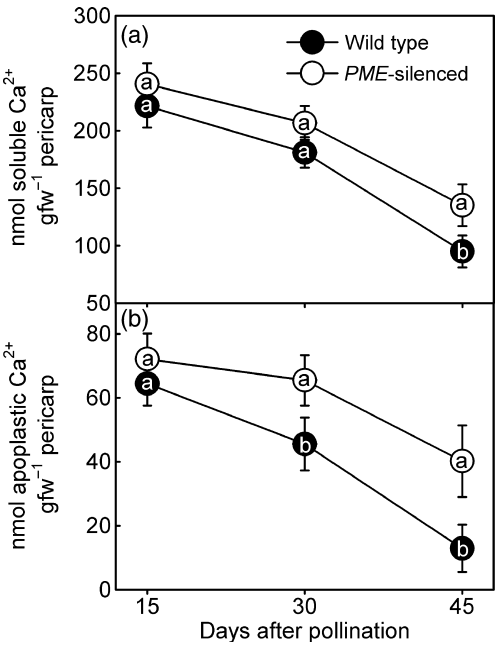

Figure 2. Silencing *PME* expression alters calcium solubility and partitioning in fruit pericarp tissue.
Total water-soluble Ca^{2+} (a) and water-soluble apoplastic Ca^{2+} (b) extracted from pericarp tissue of wild-type and *PME*-silenced tomato fruit cultivar Rutgers. gfw = grams of fresh weight. Wild-type (n = 4) and *PME*-silenced (n = 4) samples were compared with one-tailed unpaired Student's t-test. Different letters on each evaluation day represent a statistical difference between wild-type and *PME*-silenced samples (P-value < 0.05). Data are means ± standard error (SE).

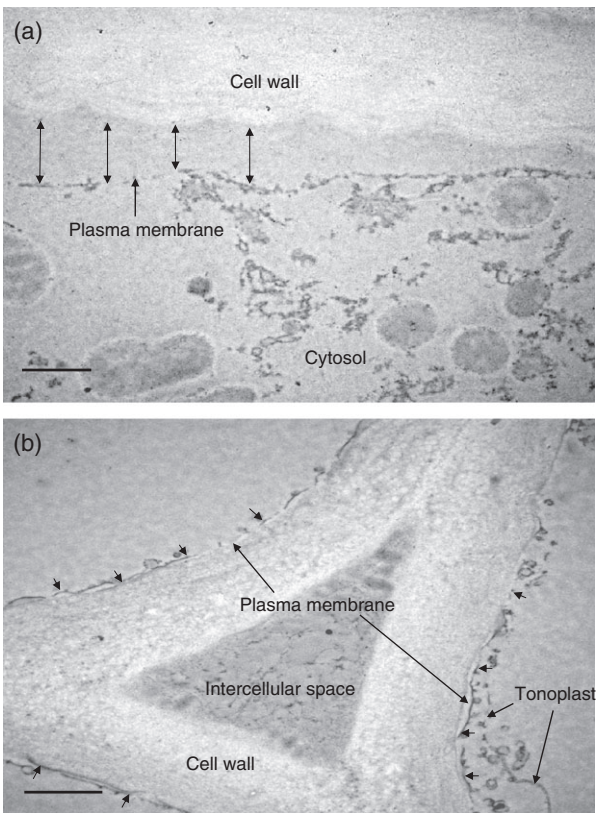

Figure 3. Electron microscopy images of subepidermal pericarp tissue of wild-type (a) and *PME*-silenced (b) 'Rutgers' tomato fruit at 45 DAP.
(a) Double arrows are showing the plasma membrane detached from the cell wall, indicating cell plasmolysis in subepidermal wild-type pericarp tissue. Scale bar, 5 μm.
(b) Arrowheads pointing to the plasma membrane pressed against the cell wall of *PME*-silenced subepidermal pericarp tissue. Scale bar, 2 μm.

42-fold lower in *PME*-silenced fruit, respectively, than in wild-type fruit at 45 DAP (Figure 4).

In situ immunolocalization and chemical analysis of pectins

In situ immunolocalization analysis of levels of pectin esterification in tomato fruit at 45 DAP shows that the cell walls of pericarp tissue of wild-type fruit contain a substantial amount of weakly esterified or unesterified pectins (i.e., pectins bound by the JIM5 monoclonal antibody) in the cell wall region close to the plasma membrane (Figure 5a). In contrast, relatively lower amounts of these weakly esterified or unesterified pectins were observed in the analogous cell wall location in pericarp tissue of *PME*-silenced fruit (Figure 5b). *In situ* analysis of heavily methylesterified pectins (i.e., those bound by the JIM7 antibody) at 45 DAP revealed a low level of these pectins in the cell wall in pericarp tissue of wild-type (Figure 6a), compared with the level in the cell wall of *PME*-silenced fruit (Figure 6b). Chemical analysis of pectin esterification in *PME*-silenced and wild-type fruit pericarp showed similar levels of pectin esterification in both the water-soluble (~35%) and insoluble (~45%) pectin fractions at 15 DAP; these levels of pectin esterification decreased

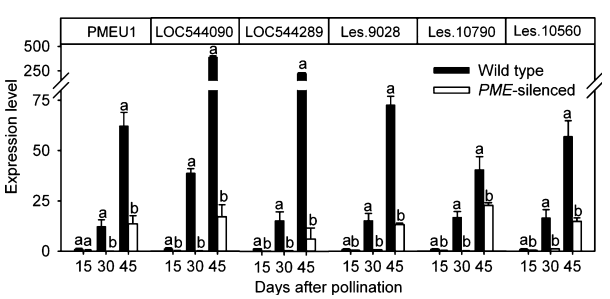

Figure 4. Changes in *PME* expression during wild-type and *PME*-silenced fruit growth and development.
The expression analysis was accomplished in pericarp tissue of wild-type and *PME*-silenced tomato fruit cultivar Rutgers for three *PME* genes (PMEU1, LOC544090, LOC544289), and three *PME* unigenes (Les.9028, Les.10790, and Les.10560). Wild-type (n = 4) and *PME*-silenced (n = 4) samples were compared by one-tailed unpaired Student's t-test. Different letters on each evaluation day represent a statistical difference between wild-type and *PME*-silenced samples (P-value < 0.05). Data are means ± standard error (SE).

markedly as wild-type 'Rutgers' fruit developed further but declined much less or not at all in *PME*-silenced fruit (Figure 7).

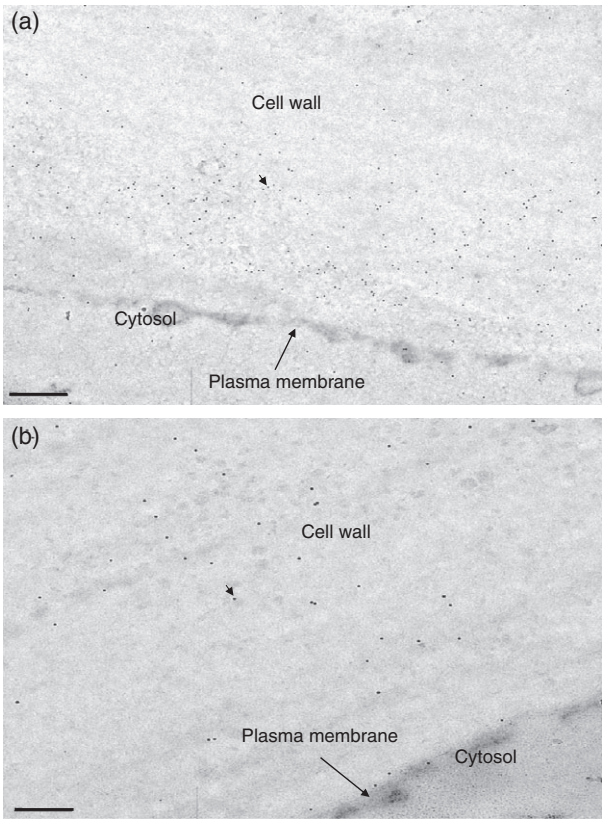

Figure 5. Immunogold labeling (10 nm gold grains) of subepidermal pericarp cells of 'Rutgers' tomato fruit at 45 DAP with JM5 antibody. Uranyl acetate counterstaining.
(a) Wild-type pericarp tissue. Scale bar, 2 μm.
(b), *PME*-silenced pericarp tissue. Scale bar, 2 μm. Black dots (indicated by arrowheads) identify the location of the binding between the monoclonal antibody JIM5 and sparsely methylated or unesterified homogalacturonan epitope.

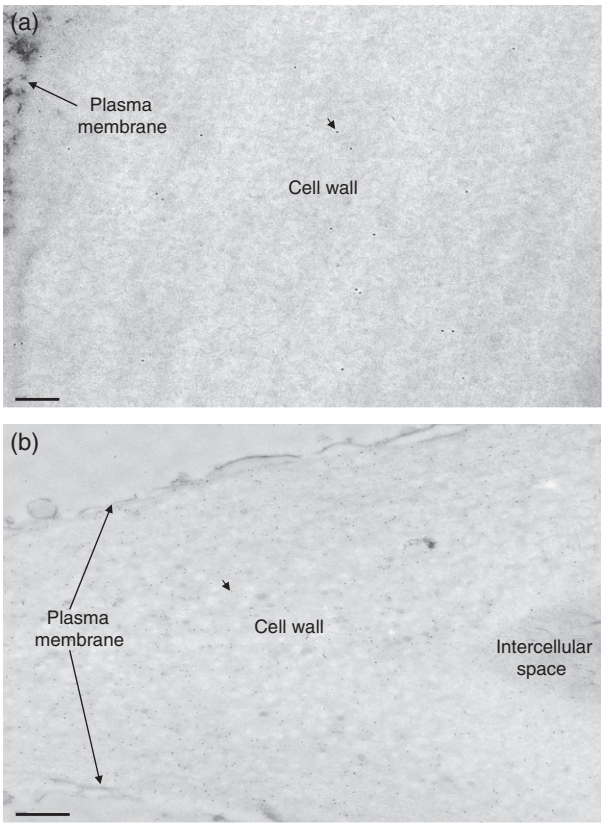

Figure 6. Immunogold labeling (10 nm gold grains) of subepidermal pericarp cells of 'Rutgers' tomato fruit at 45 DAP with the JM7 monoclonal antibody. Uranyl acetate counterstaining.
(a) Wild-type pericarp tissue. Scale bar, 0.2 μm.
(b), *PME*-silenced pericarp tissue. Scale bar, 0.5 μm. Black dots (indicated by arrowheads) identify the location of the binding between the monoclonal antibody JIM7 and heavily methylated or methylesterified homogalacturonan epitope.

Fruit and pectin-bound calcium concentrations

The total concentrations of Ca^{2+} in the pericarp tissues of wild-type and *PME*-silenced fruit decreased from 15 to 45 DAP, but the values for each fruit type were similar at each developmental time point (Figure 8a). The *PME*-silenced fruit pericarp showed a slightly lower Ca^{2+} concentration in the water-soluble pectin fraction than wild-type fruit at 45 DAP (Figure 8b). The Ca^{2+} concentrations in the water-insoluble pectin were similar in wild-type and *PME*-silenced fruit pericarp at 15 DAP and increased steadily from 30 to 45 DAP in wild-type fruit while the Ca^{2+} concentration remained unchanged in the *PME*-silenced fruit (Figure 8c).

Fruit growth and cell wall concentration

Wild-type and *PME*-silenced fruit showed statistically similar increases in fruit weight during growth and development (Figure 9a). Decreases in total cell wall concentration were also similar in wild-type and *PME*-silenced fruit tissue during growth and development (Figure 9b). We observed a consistently high rate of fruit growth. Cell wall concentration in the pericarp tissue decreased ~10% from 15 to 30 DAP and was maintained constant from 30 to 45 DAP in both wild-type and *PME*-silenced fruit (Figure 9b).

Cytosolic and vacuolar Ca^{2+} contents

Based on the analysis of cytosolic Ca^{2+} content accomplished under a confocal microscope with the fluorescent Ca^{2+} indicator Fluo-4, the steady-state cytosolic Ca^{2+} content was statistically similar between wild-type and *PME*-silenced fruit pericarp cells at 45 DAP (Figure 10). Similarly, the analysis of vacuolar Ca^{2+} content accomplished with electron microscopy with a potassium antimonate-Ca^{2+} precipitation approach revealed no visual differences between Ca^{2+} content inside the vacuole of wild-type and *PME*-silenced fruit pericarp cells at 45 DAP (Figure 11). Electron microscopy analysis also showed a higher Ca^{2+}

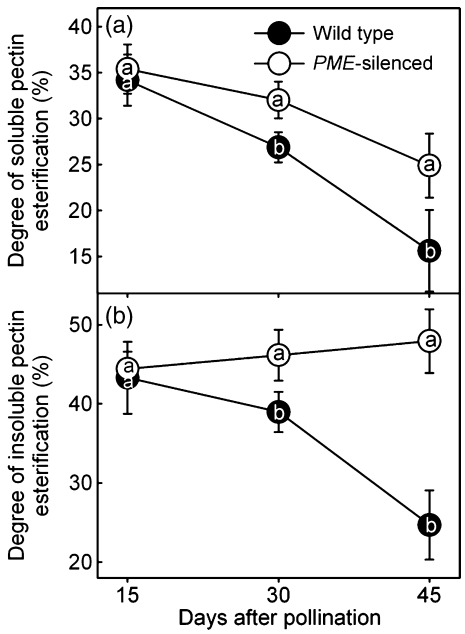

Figure 7. Changes in pectin esterification during wild-type and *PME*-silenced fruit growth and development.
Degree of esterification of water-soluble pectin (a) and water-insoluble pectin (b) fractions extracted from pericarp tissue of wild-type and *PME*-silenced tomato fruit cultivar Rutgers. Wild-type (n = 4) and *PME*-silenced (n = 4) samples were compared by one-tailed unpaired Student's t-test. Different letters on each evaluation day represent a statistical difference between wild-type and *PME*-silenced samples (P-value < 0.05). Data are means ± standard error (SE).

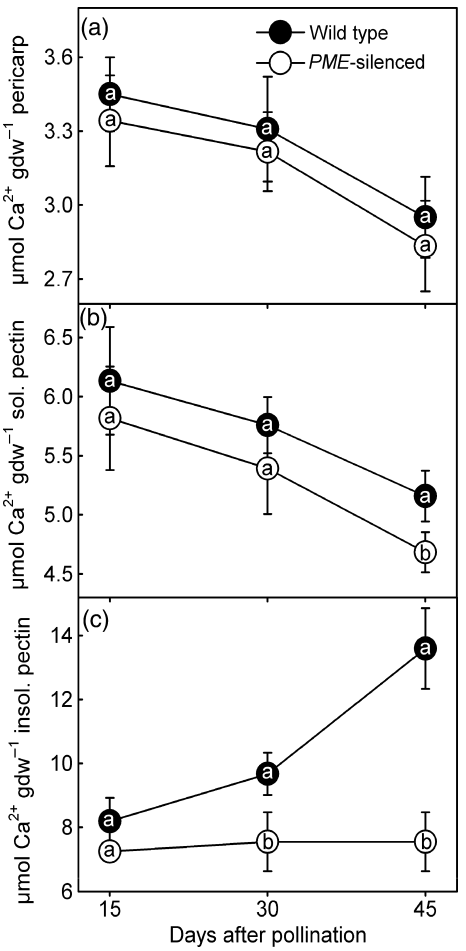

Figure 8. Silencing *PME*s decreases insoluble pectin-bound Ca^{2+} during fruit growth and development.
Calcium concentration in pericarp tissue (a), as well as in water-soluble pectin (b) and water-insoluble pectin (c) fractions extracted from pericarp tissue of wild-type and *PME*-silenced tomato fruit cultivar Rutgers. gdw = grams of dry weight. sol. = soluble, insol. = insoluble. Wild-type (n = 4) and *PME*-silenced (n = 4) samples were compared by one-tailed unpaired Student's t-test. Different letters on each evaluation day represent a statistical difference between wild-type and *PME*-silenced samples (P-value < 0.05). Data are means ± standard error (SE).

content bound to the cell wall of wild-type fruit pericarp cells compared with *PME*-silenced pericarp cells (Figure 11).

DISCUSSION

In our study, tomato was used as a model system to better understand the mechanisms involved in Ca^{2+} deficiency disorder development in plants.

Fruit susceptibility to BER is influenced by pectin de-esterification

Recently, it has been suggested that abnormal regulation of Ca^{2+} partitioning and distribution in the cell influences fruit susceptibility to BER (Ho and White, 2005). The cell wall represents the biggest pool of Ca^{2+} in the fruit tissue (Demarty *et al.*, 1984). Consequently, changes in the expression of enzymes that create binding sites for Ca^{2+} in the cell wall, such as PMEs, can potentially affect cellular Ca^{2+} partitioning and distribution. Accordingly, our results show that *PME*-silenced fruit are less susceptible to BER development, which takes places at the time that fruit Ca^{2+} uptake decreases and cells reach the highest rates of expansion, vacuolation, and dilution of Ca^{2+} content (White and Broadley, 2003; Ho and White, 2005).

Pectin de-esterification during fruit growth and cell wall biosynthesis

Although our results show high rates of fruit growth, cell wall concentration in pericarp tissue had about 10% reduction from 15 to 30 DAP and was maintained constant from 30 to 45 DAP in both wild-type and *PME*-silenced fruit. These results suggest that cell wall biosyntheses is lower at the first stage (15 to 30 DAP), and increases during the second stage (30 to 45 DAP) of fruit growth and development, which counterbalance a possible dilution of the cell wall content in response to rapid fruit expansion. During cell wall biosynthesis and assembly, the pectins secreted to the apoplast are

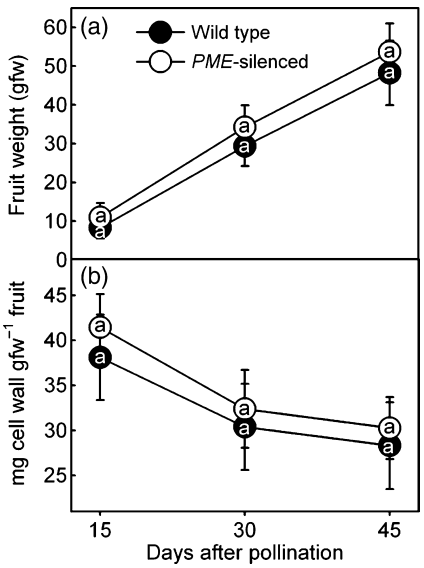

Figure 9. Dynamics of fruit growth and cell wall biosynthesis.
Average fruit weight (a) and cell wall concentration in pericarp tissue (b) of wild-type and *PME*-silenced tomato fruit cultivar Rutgers. gfw = grams of fresh weight. Wild-type (n = 4) and *PME*-silenced (n = 4) samples were compared by one-tailed unpaired Student's t-test. Different letters on each evaluation day represent a statistical difference between wild-type and *PME*-silenced samples (P-value < 0.05). Data are means ± standard error (SE).

highly esterified, and are later de-esterified by the activity of PMEs (Bosch and Hepler, 2005; Wolf *et al.*, 2009). According to the results obtained in *PME*-silenced fruit, *PME* expression increased, and the degree of water-insoluble pectin esterification was maintained constant from 15 to 45 DAP, which suggests that pectins were secreted to the apoplast at the same rates that they were de-esterified by the activity of PMEs. Accordingly, the *in situ* analysis shows equal distribution of de-esterified pectins throughout the cell wall in *PME*-silenced pericarp tissue. These results indicate that the increase in *PME* expression was parallel with the increase in pectin secretion to the apoplast in *PME*-silenced fruit tissue.

In wild-type fruit, the degree of esterification of the water-insoluble pectin decreased during fruit growth and development, which indicated that the rates of pectin de-esterification by PME activity were higher than the rates of pectin secretion to the apoplast. These results are strongly supported by the higher increase in *PME* expression observed in wild-type fruit tissue from 15 to 45 DAP, compared with that in the *PME*-silenced fruit. In addition, *in situ* analysis shows higher concentrations of pectins with a low degree of methyl esterification close to the plasma membrane in wild-type pericarp tissue, which is in agreement with the higher *PME* expression observed at later stages of fruit growth and development (30–45 DAP).

The water-soluble pectin fraction in tomato fruit is composed mostly of low-molecular-weight pectin chains created by the activity of pectin degrading enzymes that are responsible for the release of de-esterified pectins from the water-insoluble fraction into the water-soluble pectin fraction (Brummell and Harpster, 2001; Micheli, 2001). In the cell wall matrix, water-soluble pectins are possibly more accessible to PMEs than water-insoluble pectins, which could explain the correlation between increasing *PME* expression and decreasing water-soluble pectin esterification observed not only in the wild-type (r^2 = −0.95), but also in the *PME*-silenced fruit (r^2 = −0.95).

In general, the degrees of esterification of water-soluble and insoluble pectin fractions analyzed in our study were lower than previously reported in other studies (Tieman *et al.*, 1992). The lower degree of esterification of water-soluble and insoluble pectin fractions could be explained by the lower total fruit tissue Ca^{2+} concentration, compared with other studies (Tieman and Handa, 1994). Lower fruit Ca^{2+} concentration resulted in lower cell wall bound Ca^{2+} and the loosened cell wall matrix facilitated PME enzyme access to esterified pectin chains, as reported for other cell wall metabolizing enzymes (Buescher and Hobson, 1982).

Calcium binding to pectins during fruit expansion and BER development

In the cell wall, PMEs carry out block-wise de-esterification, creating contiguous stretches of galacturonic acid residues (Bosch and Hepler, 2005). The extent and strength of Ca^{2+}

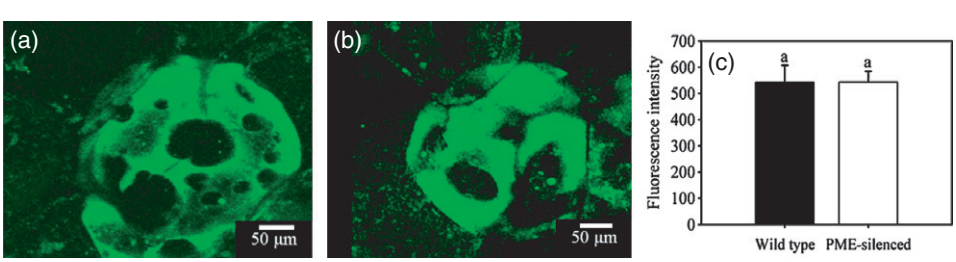

Figure 10. Projection of 3D images of Fluo-4 fluorescence in the cytosol of wild-type (a) and *PME*-silenced (b) fruit pericarp cells at 45 DAP.
Fluorescence intensities of wild-type and *PME*-silenced fruit pericarp cells (c). Higher fluorescence intensity means higher cytosolic Ca^{2+} concentration. Wild-type (n = 4) and *PME*-silenced (n = 4) samples were compared by one-tailed unpaired Student's t-test. Different letters represent a statistical difference between wild-type and *PME*-silenced samples (P-value < 0.05). Data are means ± standard error (SE). Data presented show the fluorescence intensity distribution of 12 cells from four replications (three cells per replication) of wild-type or *PME*-silenced fruit.

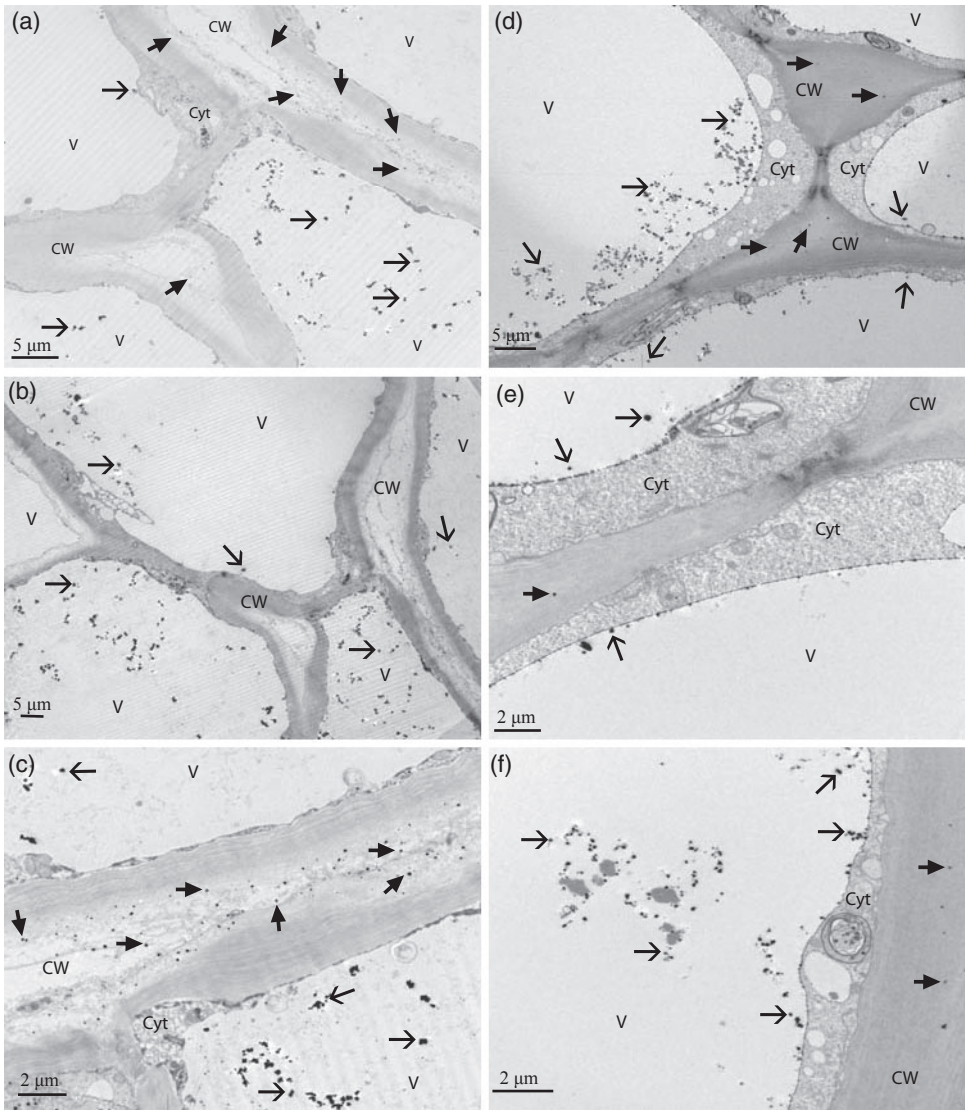

Figure 11. Electron microscopy images of wild-type (a–c) and *PME*-silenced (d–f) fruit pericarp cells without visible BER symptoms at 45 DAP.
Arrows are pointing to black spots resulting from the reaction between potassium antimonate and Ca^{2+} showing cell with Ca^{2+} accumulation inside the vacuole (a–f). Arrowheads are pointing to potassium antimonate-Ca^{2+} precipitates in the cell wall (a–f). V = vacuole, CW = cell wall, Cyt = cytosol. Images shown represent the average of 12 images taken on four single fruit replications of each genotype (three images per fruit).

cross-linking will depend on the pattern of de-esterification as well as on the number and availability of the acidic residues (Hepler and Winship, 2010). Under conditions of a low degree of block-wise de-esterification, pectins associate ionically, with carboxyl moieties participating in labile binding with free Ca^{2+}-forming plastic gels with low shear strength (Fang *et al.*, 2008). As pectins are de-esterified block-wise by PME, dimers begin to form in a cooperative fashion, so that binding strength increases rapidly as the ratio of Ca^{2+} to available binding sites increases (Hepler and Winship, 2010). The number of consecutive de-esterified galacturonic acid residues required to form stable chains in a modified, or shifted 'egg-box' configuration (Braccini and Perez, 2001; Braccini *et al.*, 2005) has been estimated in various systems to range from 6 to 20 (Fraeye *et al.*, 2009).

In our study, the decrease in insoluble pectin esterification was negatively correlated with increased Ca^{2+} bound to the insoluble pectin fraction ($r^2 = -0.99$) in wild-type fruit. In the insoluble fraction, long de-esterified pectin chains form the stable 'egg box' configuration (Demarty *et al.*, 1984; Ralet *et al.*, 2001). In contrast, the water-soluble pectin fraction is mostly comprised of short, low esterified pectin chains that have low affinity for Ca^{2+} (Thakur *et al.*, 1997; Tibbits *et al.*, 1998; Brummell and Harpster, 2001). In the *PME*-silenced fruit, the relatively constant overall pectin esterification resulted in a constant Ca^{2+} concentration in the insoluble

pectin fraction during fruit growth and development (r^2 = 0.85). Our results consistently show that Ca^{2+} concentrations in the water-soluble pectin decrease at rates similar to those in total fruit tissue and apoplastic Ca^{2+} concentrations during growth and development of wild-type and *PME*-silenced fruit. These results suggest that Ca^{2+} associated with the water-soluble pectin fraction is determined by Ca^{2+} equilibration with the fruit tissue's water-soluble apoplastic Ca^{2+} concentration. Although the water-soluble pectin may have a lower affinity for Ca^{2+} than does the insoluble pectin fraction, the lower degree of esterification of the soluble pectin fraction observed in wild-type fruit could explain the higher Ca^{2+} concentration observed in the wild-type soluble pectin fraction at 45 DAP, compared with that of the *PME*-silenced fruit.

Our results show that *PME*-silenced fruit tissues have less Ca^{2+} associated with both the water-insoluble and soluble pectins during rapid cell expansion and vacuolation. This situation should maintain higher levels of total and apoplastic water-soluble Ca^{2+} and reduce fruit susceptibility to BER development. Therefore, rapid fruit expansion associated with higher pectin biosynthesis and de-esterification could play a role in Ca^{2+} partitioning and distribution in the cell, eventually resulting in lower apoplastic Ca^{2+} concentrations that negatively affect membrane structure and integrity and increase fruit susceptibility to BER development.

Although apoplastic pH also affects Ca^{2+} binding to de-esterified pectins, previous studies have shown that apoplastic pH is maintained between 6 to 7 in pericarp tissue during tomato fruit growth and development (Ruan *et al.*, 1995; Domingos and Huber, 1999) and this figure is the pH range in which pectin carboxyl groups have the highest affinity for Ca^{2+} (Garnier *et al.*, 1993; Tibbits *et al.*, 1998). This situation would mean that apoplastic pH facilitates Ca^{2+} binding to the cell wall, possibly favoring BER development in tomato fruit.

Water-soluble apoplastic Ca^{2+} concentration affects membrane leakiness

Apoplastic Ca^{2+} ions are required to bridge phosphate and carboxylate groups of phospholipids and proteins at the plasma membrane surface, maintaining proper membrane structure and function and reducing membrane leakiness (Hanson, 1960; Clarkson and Hanson, 1980; Legge *et al.*, 1982; Kirkby and Pilbeam, 1984; Picchioni *et al.*, 1998; Hirschi, 2004). Levels of free Ca^{2+} in the apoplast must reach certain thresholds for the membrane to be effective in controlling ion selectivity (Hanson, 1960; White and Broadley, 2003). Protoplasts exposed to solutions with low concentrations of EDTA had leaky plasma membranes and cytoplasmic solutes were lost to the apoplast. This leakiness was completely and immediately reversed through the addition of Ca^{2+} to these solutions (Steveninck, 1965). Other studies indicate that the plasma membrane can be damaged if Ca^{2+} is displaced from its binding sites by other cations (Wallace *et al.*, 1966), including protons (Lund, 1970).

Our results show that high rates of fruit growth and pectin de-esterification can deplete water-soluble apoplastic Ca^{2+} concentrations without evident effects on cytosolic and vacuolar Ca^{2+} contents under conditions of low fruit Ca^{2+} uptake, which increases plasma membrane leakage and leads to cell plasmolysis and BER development. In addition, suppression of *PME* expression decreased the amount of pectin-bound Ca^{2+} and maintained higher water-soluble apoplastic Ca^{2+} concentrations, possibly increasing the amount of membrane bound Ca^{2+}, which resulted in lower membrane leakiness and reduced fruit susceptibility to BER. These results suggest that *in muro* carboxyl groups of de-esterified pectins form very strong intermolecular interactions with Ca^{2+} and compete with phosphate and carboxylate groups of phospholipids and proteins on the plasma membrane for Ca^{2+} available in the apoplast. The immunolocalization analysis shows a high accumulation of low esterified pectins close to the plasma membrane, which may represent a potentially higher sink for unbound apoplastic Ca^{2+} at the plasma membrane surface region. These results are in agreement with previous studies showing that a fruit's Ca^{2+} requirement increases during stages of intensive cell expansion (Ho and White, 2005). Higher cell expansion requires higher amounts of Ca^{2+} to maintain proper membrane structure and function and supply Ca^{2+} to the growing vacuole that represents about 40% of total tissue Ca^{2+} content (Harker and Venis, 1991).

Cytosolic and vacuolar Ca^{2+} content with suppression of *PME* expression

Although silencing *PME* expression maintained higher water-soluble apoplastic Ca^{2+}, it showed no effect on cytosolic and vacuolar pools of Ca^{2+}. The water-soluble apoplastic Ca^{2+} is in direct contact with the cell wall matrix, and is expected to change in response to changes in Ca^{2+} binding to the cell wall. Cytosolic and vacuolar Ca^{2+} concentrations are known to be highly regulated by a sophisticated system including Ca-ATPases, Ca^{2+}/H^+ exchangers, and Ca^{2+} channels that ensure appropriate levels of Ca^{2+} are maintained in these cellular compartments (White and Broadley, 2003). In this way, the observed changes in cell wall and water-soluble apoplastic Ca^{2+} content were not sufficient to affect the regulation of Ca^{2+} distribution in the cytosolic and vacuolar compartments. In this context, it is interesting to note that, whereas vacuolar Ca^{2+} storage has been shown to regulate apoplastic Ca^{2+} concentration (Conn *et al.*, 2011; De Freitas *et al.*, 2011), an alteration in the apoplastic free [Ca^{2+}], such as that caused by the suppression of *PME* expression, does not seem to affect vacuolar [Ca^{2+}].

Cell wall Ca^{2+} binding capacity can determine water-soluble apoplastic Ca^{2+} levels and fruit susceptibility to BER

Previous studies have shown cell wall thickening in fruit tissues with Ca^{2+} deficiency symptoms (Simons and Chu, 1983) and have suggested that lower levels of Ca^{2+} bound to the cell wall could be the cause of Ca^{2+} deficiency development (Ho and White, 2005). Our results show that higher cell wall Ca^{2+} binding capacity can cause a depletion of water-soluble apoplastic Ca^{2+} and an increase in fruit susceptibility to BER. Plants that have more binding sites for Ca^{2+} in the cell wall are known to require higher levels of Ca^{2+} for normal growth and development. For instance, dicotyledonous plants require more Ca^{2+} in their tissues than monocotyledonous plants (Islam *et al.*, 1987), a phenomenon attributed to the larger cation exchange capacity of their cell walls (Kirkby and Pilbeam, 1984). Therefore, susceptibility of tomato genotypes to BER development may be determined by the capacity of their cell walls to bind Ca^{2+} during rapid cell expansion and vacuolation under conditions in which fruit Ca^{2+} uptake is restricted. Comparative analysis of Ca^{2+} binding to the cell wall during BER development in more and less susceptible tomato genotypes could be used to further elucidate the role of the cell wall on BER development. In this context, breeding for reduced *PME* expression is a potential tool to reduce Ca^{2+} binding to the cell wall and fruit susceptibility to BER. Previous studies have shown that silencing fruit specific *PME* expression does not affect fruit softening processes during ripening, implying that selecting fruit with low *PME* expression will not cause trade-offs in fruit quality after harvest (Tieman and Handa, 1994).

EXPERIMENTAL PROCEDURES

Experimental approach

The experiment was accomplished two times. Wild-type and *PME*-silenced tomato plants (*Solanum lycopersicum*) cultivar Rutgers were grown in 9.5 L pots containing 0.3 kg of perlite as substrate in a greenhouse environment. The *PME*-silenced plants (line 3781^) contain two copies of a *PME* type I antisense nucleotide sequence (GenBank: U70676.1) under the control of the cauliflower mosaic virus 35S promoter (Tieman *et al.*, 1992). Both wild-type and *PME*-silenced plants were irrigated every day with a nutrient solution containing N (102 mg L^{-1}), P (26 mg L^{-1}), K (124 mg L^{-1}), Ca^{2+} (90 mg L^{-1}), Mg^{2+} (24 mg L^{-1}), S (16 mg L^{-1}), Fe (1.6 mg L^{-1}), Mn (0.27 mg L^{-1}), Cu (0.16 mg L^{-1}), Zn (0.12 mg L^{-1}), B (0.26 mg L^{-1}), and Mo (0.016 mg L^{-1}). After tagging and manually pollinating the flowers at full bloom, the plants were irrigated everyday with the same nutrient solution, but without Ca^{2+}. There were four replications with four plants each for wild-type and *PME*-silenced plants. Fruit from the first and second clusters on each plant were harvested and analyzed at 15, 30, and 45 DAP. All tissue analyses were accomplished in fruit without visible BER symptoms using blossom-end tissue.

Blossom-end rot incidence and fruit weight

The BER incidence was determined by counting the number of tagged fruit with BER symptoms, dividing by the total number of tagged fruit, and multiplying by 100. Fruit fresh weight was determined by dividing the total tagged fruit weight by the total number of tagged fruit in each replication.

Electrolyte leakage and total water-soluble Ca^{2+}

Electrolyte leakage was determined in three pericarp fruit discs of 1 cm diameter and 0.5 cm thickness without epidermis (≈3 g fw). One disc cut from each of three fruit represented one replication, which was placed into a 50 ml conical tube containing an isotonic mannitol solution (0.68 MPa), and the conductivity was recorded during 6 h at 20°C on a rotary shaker at 60 rpm. After 6 h, the samples were frozen and thawed twice to determine total conductivity (Saltveit, 2002). Electrolyte leakage was calculated based on the change in conductivity per hour as a percentage of the total conductivity. Each replication was filtered and the solution used to determine the total tissue water-soluble Ca^{2+}.

Apoplastic water-soluble Ca^{2+}

Twelve pericarp fruit discs of 1 cm diameter and 0.5 cm thickness without epidermis (total ≈12 g fw) were used for apoplastic Ca^{2+} extraction. Each sample of 12 discs, one disc from each of three fruit from each of four plants, represented one replication. After cutting, each disc was rinsed in deionized water for 10 sec and blotted dry. Each disc was then placed in a funnel that contained a flat acrylic membrane (1.2 cm diameter) with pore size of 10–16 μm (Kimax®, Kimble, Vineland, NJ, USA). The funnel was fitted over a Kitasato flask (Pyrex®, Lowell, MA,USA), and 10–15 Hg of vacuum was applied. A 0.68 MPa mannitol solution was slowly dripped over the entire disc surface (500 μl) and collected in the Kitasato flask for Ca^{2+} quantification. The entire procedure was accomplished at 4°C. Cell damage was not detected under a light microscope Olympus SZH10 (America Inc., Lake Success, NY, USA) by analyzing samples before and after the extraction of water-soluble apoplastic Ca^{2+} extraction.

Quantitative real-time polymerase chain reaction (qPCR)

Total RNA was extracted from pericarp tissue with epidermis using RNeasy Plant Mini Kit (Qiagen, Valencia, CA, USA). About 3 μg of RNA was reverse transcribed using SuperScript III (Invitrogen, Carlsbad, CA, USA). Quantitative RT-PCR was then performed with the addition of 1xSYBR green (Applied Biosystem, Foster City, CA, USA) to each sample containing about 100 ng of the synthesized cDNA. The data were normalized based on the expression of the tomato 18S rRNA (Martinelli *et al.*, 2009). *Pectin methylesterase* is a small gene family in tomato, some members of which are highly homologous (Alexander and Grierson, 2002). In our study, the expression analysis was accomplished for three tomato *PME* genes (PMEU1, LOC544090, LOC544289), and three tomato *PME* unigenes (Les.9028, Les.10790, and Les.10560). The nucleotide sequences of *PME* genes were obtained from previous studies (Hall *et al.*, 1994; Thanh *et al.*, 2007), whereas the nucleotide sequences of *PME* unigenes were obtained by assembling expressed sequence tags (ESTs) together. The Les.9028 unigene has 89.3% identity to PME (NCBI: XP_002278061.1), Les.10790 unigene has 60.2% identity to PME (NCBI: XP_002321999.1), and Les.10560 has 52.6% identity to PME (XP_002321999.1). All nucleotide sequences were obtained from the NCBI database (http://www.ncbi.nlm.nih.gov/Genbank/). The ID numbers and designed primers are specified in Table S1 on-line.

Cell wall extraction and analysis

Pericarp tissue with skin excised from the blossom-end half of sound wild-type and *PME*-silenced tomato fruit were stored at −80°C and used for cell wall extraction according to Campbell *et al.*

(1990). The total cell wall extracted was freeze-dried, weighed and then suspended in distilled H_2O for 1 h and centrifuged (10 500 ***g***, 25 min). The supernatant was collected and the water extraction step was repeated once. The two supernatants were combined and designated as the water-soluble pectin fraction. The remaining pellet was considered to contain the water-insoluble pectin fraction. Both water-soluble and -insoluble fractions were freeze-dried weighed and analyzed for degree of pectin esterification and Ca^{2+} concentration. The total uronic acid content of each pectin fraction was measured based on the method described by Ahmed and Labavitch (1977). The degree of esterification was measured by the reductive method in which the esterified galacturonosyl carboxyl groups are reduced (i.e., converted from galacturonic acid to galactose) and then the difference in uronic acid contents of reduced and untreated samples represents the amount of uronosyl residues in the original sample that had been esterified (Klein *et al.*, 1995). Pectin samples were incubated overnight at room temperature in 1 ml of 10 mg ml^{-1} $NaBH_4$ in 50% ethanol plus 50% NaOH (0.5%). The reduced samples were then neutralized with acetic acid (HOAc), dried, and washed several times with HOAc: methanol (MeOH) (1:9) and then MeOH. Later, reduced and unreduced samples were dissolved in 67% H_2SO_4 and the unesterified uronic acid content determined spectrophotometrically (Blumenkrantz and Asboe-Hansen, 1973; Ahmed and Labavitch, 1977).

Calcium quantification

Calcium was analyzed in liquid (apoplastic and total soluble Ca^{2+}) and freeze-dried water-soluble pectin, water-insoluble pectin, and pericarp tissue with skin cut at the blossom end of the fruit. All samples were subjected to microwave acid digestion/dissolution and analyzed for Ca^{2+} by inductively coupled plasma-atomic emission spectrometry, as described by Meyer and Keliher (1992).

Pectin *in situ* immunolocalization assays

Pieces (2–3 mm^3) of pericarp tissue that contained the skin were excised at the blossom-end region of healthy wild-type and *PME*-silenced tomato fruit at 45 DAP. After cutting, the samples were fixed in a modified Karnovsky's fixative (Karnovsky, 1965) that contained 2% glutaraldehyde and 2.5% formaldehyde in 0.1 M potassium phosphate buffer, pH 7.6 for 6 h at 20°C in total darkness. Samples were then incubated in 0.1% tannic acid in 0.1 M phosphate buffer for 30 min at 20°C. After being partially dehydrated in a graded aqueous ethanol series with 30% and 50% ethanol for 10 min each concentration, samples were incubated in 2% uranyl acetate in 50% ethanol for 60 min at 20°C, following further dehydration in 75, 95, and 100% ethanol for 10 min each concentration. Samples were infiltrated overnight with 50:50 (100% ethanol:London Resin White (LRW) (London Resin Co., London, UK). Each sample was then infiltrated for 2 h with 100% LRW at 20°C. The resin was polymerized in a vacuum oven set (55°C for 24 h). Semi-thin sections (1 μm thick) of pericarp with skin were prepared and mounted on 100 mesh *Formvar-coated gold grids (Ted* Pella, Inc., Redding, CA, USA). Wild-type and *PME*-silenced tomato fruit samples mounted in the grids were incubated in 0.01 M phosphate-buffered saline (PBS) that contained 1% fish gelatin at pH 7.2 for 30 min at 20°C. Grids containing the samples were then blotted dry and incubated overnight at 4°C with the rat monoclonal antibodies JIM5 or JIM7 diluted 1:4 (v/v) in 0.01 M PBS. JIM5 binds to a sparsely methylated and unesterified homogalacturonan epitope, whereas JIM7 binds to a heavily methylesterified pectin epitope (Knox *et al.*, 1990; Willats *et al.*, 2000; Clausen *et al.*, 2003). Each sample was then rinsed with 15 ml of PBS (0.01 M), blotted dry and incubated for 1 h at 20°C in a goat anti-rat polyclonal antibody gold conjugate with 10 nm colloidal gold complexes (*Ted* Pella, Inc., Redding, CA, USA). The polyclonal secondary antibody was diluted 1:50 in PBS (0.01 M). The grids containing the samples were then washed dropwise with 15 ml of distilled water, and blotted dry. After washing, the grids were stained with 1% uranyl acetate. Grids that contained wild-type and *PME*-silenced fruit tissue were then analyzed under a Philips CM120 Biotwin Lens electron microscope at 75 kV (F.E.I. Company, Hillsboro, OR, USA) for *in situ* immunolocalization of sparsely and heavily methylated pectins.

Cytosolic Ca^{2+} content

Cytosolic Ca^{2+} content was analyzed in four fruit replications as described by De Freitas *et al.* (2011). Each replication was a single fruit harvested from each of four wild-type or *PME*-silenced plants at 45 DAP. From each fruit, three thin, healthy subepidermal pericarp sections were manually cut from the blossom-end region. Thin sections were then incubated in a loading solution containing 100 mM KCl, 10 mM MES (pH 5.0 with KOH), 1 mM $CaCl_2$, 300 μM eserine, and 5 μM Fluo-4:acetoxymethyl ester (Fluo4-AM) (Invitrogen, Carlsbad, CA, USA) for 1 h. The negative control samples were incubated in 100 mM KCl, 10 mM MES (pH 5.0 with KOH), 300 μM eserine, 5 μM Fluo4-AM with 5 mM ethylene glycol tetraacetic acid (EGTA) and 25 μM A23187 (Supplemental Figure 1). A23187 is an ionophore, which permits the free movement of $[Ca^{2+}]$ across the hydrophilic plasma membrane. The EGTA can eliminate the extracellular free $[Ca^{2+}]$, then the intracellular $[Ca^{2+}]$ will be moved to the outside of the cell with the help of A23187 due to the $[Ca^{2+}]$ gradient across the plasma membrane. Therefore, the cytosolic $[Ca^{2+}]$ concentration can be decreased to an extremely low level. The fluorophores were imaged using a Zeiss LSM 5 PASCAL confocal microscope with 488 nm argon laser excitation, 488 nm dichroic mirror, 505–530 nm band-path emission filter, 10 × 0.3 numerical aperture, and Neofluar objective lense (Zeiss, Welwyn Garden City, UK). The pinhole setting was Air unit = 1. All cell images were taken under the exact same conditions and during the same session. In each sample, cells were optically sectioned and the images obtained were used to generate 3-D projection images using the brightest point projection method in the Zeiss LSM 5 PASCAL software. The edge of each cell 3-D projection image was manually delineated, and the average fluorescence intensity of the cell quantified using the Image-J program. The average fluorescence intensities were determined in a total of 12 cells in each genotype. The fluorescence intensity of each replication represents the average of the fluorescence intensity of three cells measured in each of four fruit.

Vacuolar Ca^{2+} content

Vacuolar Ca^{2+} content was determined in four single fruit replications of wild-type and *PME*-silenced genotype at 45 DAP as described by De Freitas *et al.* (2011). From each fruit, three healthy pericarp sections were manually cut from the blossom-end region. Pericarp section was then fixed in 4% glutaraldehyde in 0.1 M potassium phosphate buffer (pH 7.2) that contained 2% potassium antimonate. After rinsing in buffer (0.1 M phosphate buffer that contained 2% potassium antimonate, pH 7.2), the tissue was post fixed in 1% osmium tetroxide in 0.1 M potassium phosphate buffer that contained 2% potassium antimonate for 2 h at 4°C. The tissue was dehydrated in a graded alcohol series and embedded in epoxy resin. For observation with the transmission electron microscope, ultrathin sections were prepared. Control grids mounted with tissue sections were immersed in a solution of 100 mM EGTA (pH 8.0), a chelator with high affinity for Ca^{2+}, and incubated at 60°C for 1 h (Supplemental Figure 2). After treatment, the grids were rinsed in

distilled water (Suzuki *et al*., 2003). Electron micrographs were taken with a Philips CM120 Biotwin Lens electron microscope at 75 kV (F.E.I. Company, Hillsboro, OR). All samples were exposed to the same buffers, as well as processed and analyzed at the same time.

Statistical analysis

Statistical differences between wild-type and *PME*-silenced tomato samples were calculated with one-tailed unpaired Student's *t*-test. *P*-values <0.05 were considered significant. The normality of the data was analyzed with the Statistical Analysis System (SAS) software (SAS Institute, 2002). Data are presented as means ± standard error (SE). The Pearson's Correlation Coefficient (*r*) was calculated for the parameters *PME* expression (average of all six *PMEs*) × -water-soluble pectin esterification, and water-insoluble pectin esterification × water-insoluble pectin Ca^{2+} content for both wild-type and *PME*-silenced fruit.

ACKNOWLEDGEMENTS

We acknowledge funding from CAPES Foundation, a federal agency under the Ministry of Education of Brazil, which awarded a Fulbright Scholarship to Sergio Tonetto de Freitas for his PhD program at the University of California-Davis. We thank Dr John M. Labavitch, who contributed valuable comments and suggestions to improve the quality of this manuscript. The Complex Carbohydrate Research Center provided the monoclonal antibodies JIM5 and JIM7. Development and distribution of these antibodies is supported in part by NSF grants DBI-0421683 and RCN-0090281. The authors would also like to thank Grete Adamson, Patricia Kysar, and Emma Lee at the Electron Microscopy Laboratory, Department of Pathology and Laboratory Medicine, School of Medicine, University of California, Davis for their valuable contributions to the electron microscopy approaches used in our study. The author and co-authors have no conflict of interest to declare.

SUPPORTING INFORMATION

Additional Supporting Information may be found in the on-line version of this article:

Figure S1. Negative confocal microscopy control images of wild-type (A, B, C) and *PME*-silenced (D, E, F) fruit pericarp cells at 45 DAP. Green channel (A and D). White channel (B and E). Overlapping of Fluo-4 fluorescence and white channel images (C and F).

Figure S2. Negative electron microscopy pictures showing pericarp cell of wild-type (A) and *PME*-silenced (B) tomato pericarp at 45 DAP treated with EGTA to remove Ca^{2+} from the potassium antimonate-Ca precipitates (black spots). Arrows pointing to structures similar to the antimonate-Ca precipitates observed inside the vacuole of cells without EGTA treatment. V = vacuole, CW = cell wall, Cyt = cytosol.

Table S1. Primer sequences used for expression analysis of *PME* genes.

Please note: As a service to our authors and readers, this journal provides supporting information supplied by the authors. Such materials are peer-reviewed and may be re-organized for online delivery, but are not copy-edited or typeset. Technical support issues arising from supporting information (other than missing files) should be addressed to the authors.

REFERENCES

Ahmed, E.R.A. and Labavitch, J.M. (1977) A simplified method for accurate determination of cell wall uronide content. *J. Food Biochem.* **1**, 361–365.

Alexander, L. and Grierson, D. (2002) Ethylene biosynthesis and action in tomato: a model for climacteric fruit ripening. *J. Exp. Bot.* **53**, 2039–2055.

Blumenkrantz, N. and Asboe-Hansen, G. (1973) New method for quantitative determination of uronic acids. *Anal. Biochem.* **54**, 484–489.

Bosch, M. and Hepler, P.K. (2005) Pectin methylesterases and pectin dynamics in pollen tubes. *Plant Cell*, **17**, 3219–3226.

Braccini, I. and Perez, S. (2001) Molecular basis of Ca^{2+}-induced gelation in alginates and pectins: the egg-box model revisited. *Biomacromolecules*, **2**, 1089–1096.

Braccini, I., Rodriguez-Carvajal, M.A. and Perez, S. (2005) Chain–chain interactions for methyl polygalacturonate: models for high methylesterified pectin junction zones. *Biomacromolecules*, **6**, 1322–1328.

Brummell, D.A. and Harpster, M.H. (2001) Cell wall metabolism in fruit softening and quality and its manipulation in transgenic plants. *Plant Mol. Biol.* **47**, 311–340.

Buescher, R.W. and Hobson, G.E. (1982) Role of calcium and chelating agents in regulating the degradation of tomato fruit tissue by polygalacturonase. *J. Food Biochem.* **6**, 147–160.

Campbell, A.D., Huysamer, M., Stotz, H.U., Greve, L.C. and Labavitch, J.M. (1990) Comparison of ripening processes in intact tomato fruit and excised pericarp discs. *Plant Physiol.* **94** 1582–1589.

Castro, P.R.C. (1980) Plant growth regulators in tomato crop production. *Acta Hort.* **100**, 99–104.

Chamberlain, E.E. (1933) Blossom-end rot of tomatoes. *New Zealand J. Agric.* **46**, 293–296.

Clarkson, D.T. and Hanson, J.B. (1980) The mineral nutrition of higher plants. *Annu. Rev. Plant Physiol.* **31**, 239–298.

Clausen, M.H., Willats, W.G.T. and Knox, J.P. (2003) Synthetic methyl hexagalacturonate hapten inhibitors of anti-homogalacturonan monoclonal antibodies LM7, JIM5, and JIM7. *Carbohydr. Res.* **338**, 1797–1800.

Conn, S.J., Gilliham, M., Athman, A. *et al.* (2011) Cell-specific vacuolar calcium storage mediated by *CAX1* regulates apoplastic calcium concentration, gas exchange, and plant productivity in *Arabidopsis*. *Plant Cell*, **23**, 240–257.

De Freitas, S.T., Padda, M., Wu, Q., Park, S. and Mitcham, E.J. (2011) Dynamic alternations in cellular and molecular components during blossom-end rot development in tomatoes expressing *sCAX1,* a constitutive active Ca^{2+}/H^{+} antiporter from Arabidopsis. *Plant Physiol.* **156**, 844–855.

Demarty, M., Morvan, C. and Thellier, M. (1984) Calcium and the cell wall. *Plant, Cell Environ.* **7**, 441–448.

Domingos, P.F.A. and Huber, D. (1999) Apoplastic pH and inorganic ion levels in tomato fruit: a potential means for regulation of cell wall metabolism during ripening. *Physiol. Plant.* **105**, 506–512.

Fang, Y., Al-Assaf, S., Phillips, G.O., Nishinari, K., Funami, T. and Williams, P.A. (2008) Binding behavior of calcium to polyuronates: comparison of pectin with alginate. *Carbohydr. Polym.* **72**, 334–341.

Fraeye, I., Doungla, E., Duvetter, T., Moldenaers, P., Van Loey, A. and Hendrickx, M. (2009) Influence of intrinsic and extrinsic factors on rheology of pectin-calcium gels. *Food Hydrocoll*, **23**, 2069–2077.

Garnier, C., Axelos, M.A.V. and Thibault, J.F. (1993) Phase diagrams of pectin-calcium systems: influence of pH, ionic strength, and temperature on the gelation of pectins with different degrees of methylation. *Carbohydr. Res.* **240**, 219–232.

Hall, L.N., Bird, C.R., Picton, S., Tucker, G.A., Seymour, G.B. and Grierson, D. (1994) Molecular characterisation of cDNA clones representing pectin esterase isozymes from tomato. *Plant Mol. Biol.* **25**, 313–318.

Hanson, J.B. (1960) Impairment of respiration, ion accumulation, and ion retention in root tissue treated with ribonuclease and ethylenediamine tetraacetic acid. *Plant Physiol.* **35**, 372–379.

Harker, F.R. and Venis, M.A. (1991) Measurement of intracellular and extracellular free calcium in apple fruit cells using calcium-selective microelectrodes. *Plant, Cell Environ.* **14**, 525–530.

Harriman, R.W., Tieman, D.M. and Handa, A.K. (1991) Molecular cloning of tomato pectin methylesterase gene and its expression in Rutgers, Ripening Inhibitor, Nonripening, and Never Ripe tomato fruits. *Plant Physiol.* **97**, 80–87.

Hepler, P.K. (2005) Calcium: a central regulator of plant growth and development. *Plant Cell*, **17**, 2142–2155.

Hepler, P.K. and Winship, L.J. (2010) Calcium at the cell wall-cytoplast interface. *J. Integr. Plant Biol.* **52**, 147–160.

Hirschi, K.D. (2004) The calcium conundrum. Both versatile nutrient and specific signal. *Plant Physiol.* **136**, 2438–2442.

Ho, L.C. and White, P.J. (2005) A cellular hypothesis for the induction of blossom-end rot in tomato fruit. *Ann. Bot.* **95**, 571–581.

Ho, L.C., Belda, R., Brown, M., Andrews, J. and Adams, P. (1993) Uptake and transport of calcium and the possible causes of blossom-end rot in tomato. *J. Exp. Bot.* **44**, 509–518.

Islam, A.K.M.S., Asher, C.J. and Edwards, D.G. (1987) Response of plants to calcium concentration in flowing solution culture with chloride or sulphate as the counter-ion. *Plant Soil*, **98**, 377–395.

Karnovsky, M.J. (1965) A formaldehyde-glutaraldehyde fixative of high osmolarity for use in electron microscopy. *J. Cell Biol.* **27**, 137.

Kirkby, E.A. and Pilbeam, D.J. (1984) Calcium as a plant nutrient. *Plant, Cell Environ.* **7**, 397–405.

Klein, J.D., Hanzon, J., Irwin, P.L., Ben-Shalom, N. and Lurie, S. (1995) Pectin esterase activity and pectin methyl esterification in heated 'Golden Delicious' apples. *Phytochemistry*, **39**, 491–494.

Knox, J.P., Linstead, P.J., King, J., Cooper, C. and Roberts, K. (1990) Pectin esterification is spatially regulated both within cell walls and between developing tissues of root apices. *Planta*, **181**, 512–521.

Legge, R.L., Thompson, J.E., Baker, J.E. and Lieberman, M. (1982) The effect of calcium on the fluidity of phase properties of microsomal membranes isolated from postclimacteric golden delicious apples. *Plant Cell Physiol.* **23**, 161–169.

Lund, Z.F. (1970) The effect of calcium and its relation to several cations in soybean root growth. *Proc. Soil Sci. Soc. Amer.* **34**, 456–459.

Martinelli, F., Uratsu, S.L., Reagan, R.L., Chen, Y., Tricoli, D., Fiehn, O., Rocke, M., Gasser, C.S. and Dandekar, A.M. (2009) Gene regulation in parthenocarpic tomato fruit. *J. Exp. Bot.* **60**, 3873–3890.

Meyer, G.A. and Keliher, P.N. (1992) An overview of analysis by inductively coupled plasma-atomic emission spectrometry. In *Inductively coupled plasmas in analytical atomic spectrometry*. (Montaser, A. and Golightly, D.W., eds). New York: VCH Publishers Inc., pp. 473–516.

Micheli, F. (2001) Pectin methylesterases: cell wall enzymes with important roles in plant physiology. *Trends Plant Sci.* **6**, 414–419.

Nonami, H., Fukuyama, T., Yamamoto, M., Yang, L. and Hashimoto, Y. (1995) Blossom-end rot of tomato plants may not be directly caused by calcium deficiency. *Acta Hort.* **396**, 107–114.

Paiva, E.A.S., Martinez, H.P., Casali, V.W.D. and Padilha, L. (1998) Occurrence of blossom-end rot in tomato as a function of calcium dose in the nutrient solution and air relative humidity. *J. Plant Nutr.* **21**, 2663–2670.

Picchioni, G.A., Watada, A.E., Conway, W.S., Whitaker, B.D. and Sams, C.E. (1998) Postharvest calcium infiltration delays membrane lipid catabolism in apple fruit. *J. Agric. Food Chem.* **46**, 2452–2457.

Ralet, M.C., Dronnet, V., Buchholt, H.C. and Thibaulta, J.F. (2001) Enzymatically and chemically de-esterified lime pectins: characterization, polyelectrolyte behavior and calcium binding properties. *Carbohydr. Res.* **336**, 117–125.

Ruan, Y.L., Mate, C., Patrick, J.W. and Brady, C.J. (1995) Non-destructive collection of apoplastic fluid from developing tomato fruit using a pressure dehydration procedure. *Aust. J. Plant Physiol.* **22**, 761–769.

Saltveit, M.E. (2002) The rate of ion leakage from chilling-sensitive tissue does not immediately increase upon exposure to chilling temperatures. *Postharvest Biol. Technol.* **26**, 295–304.

SAS Institute (2002) *Statistical Analysis System, v.8.2.* Cary, NC: SAS Institute.

Saure, M.C. (2001) Blossom-end rot of tomato (*Lycopersicon esculentum* Mill.)–a calcium or a stress-related disorder? *Sci. Hort.* **90**, 193–208.

Simons, R.K. and Chu, M.C. (1983) Anomalous characteristics of cellular structure related to corking in apples. *Sci. Hort.* **19**, 113–124.

Steveninck, R.F.M.V. (1965) The significance of calcium on the apparent permeability of cell membranes and the effects of substitution with other divalent ions. *Physiol. Plant.* **18**, 54–69.

Suzuki, K., Shono, M. and Egawa, Y. (2003) Localization of calcium in the pericarp cells of tomato fruits during the development of blossom-end rot. *Protoplasma*, **222**, 149–156.

Thakur, B.R., Singh, R.K. and Handa, A.K. (1997) Chemistry and uses of pectin–A Review. *Crit. Rev. Food Sci. Nutr.* **37**, 47–73.

Thanh, D.P., Bo, W., West, G., Lycett, G.W. and Tucker, G.A. (2007) Silencing of the major salt-dependent isoform of pectinesterase in tomato alters fruit softening. *Plant Physiol.* **144**, 1960–1967.

Tibbits, C.W., MacDougall, A.J. and Ring, S.G. (1998) Calcium binding and swelling behavior of a high methoxyl pectin gel. *Carbohydr. Res.* **310**, 101–107.

Tieman, D.M. and Handa, A.K. (1994) Reduction in pectin methylesterase activity modifies tissue integrity and cation levels in ripening tomato (*Lycopersicon esculentum* Mill.) fruits. *Plant Physiol.* **106**, 429–436.

Tieman, D.M., Harriman, R.W., Ramamohan, G. and Handa, A.K. (1992) An antisense pectin methylesterase gene alters pectin chemistry and soluble solids in tomato fruit. *Plant Cell*, **4**, 667–679.

Uozumi, A., Ikeda, H., Hiraga, M., Kanno, H., Nanzyo, M., Nishiyama, M., Kanahama, K. and Kanayama, Y. (2012) Tolerance to salt stress and blossom-end rot in an introgression line, IL8-3, of tomato. *Sci Hort.* **138**, 1–6.

Wallace, A., Frohlich, E. and Lunt, O.R. (1966) Calcium requirements of higher plants. *Nature*, **209**, 634.

Wedgworth, H.H., Neal, D.C. and Wallace, J.M. (1926) Wilt and Blossom-End Rot of the Tomato; Raymond Branch Exp. Station: Raymond, MS, Bull. No. 247.

White, P.J. and Broadley, M.R. (2003) Calcium in plants. *Ann. Bot.* **92**, 487–511.

Willats, W.G.T., Limberg, G., Buchholt, H.C., Van Alebeek, G.J., Benen, J., Christensen, T.M.I.E., Visser, J., Voragen, A., Mikkelsen, J.D. and Knox, J.P. (2000) Analysis of pectic epitopes recognized by hybridoma and phage display monoclonal antibodies using defined oligosaccharides, polysaccharides, and enzymatic degradation. *Carbohydr. Res.* **327**, 309–320.

Wolf, S., Mouille, G. and Pelloux, J. (2009) Homogalacturonan methyl-esterification and plant development. *Mol. Plant*, **2**, 851–860.

